sustainability

MDPI

Article

Time-Dependent Deformation and Long-Term Strength of Carbonaceous Mudstone under Dry and Wet Cycles

Sheng-Nan Li [1,2,*], Zhu Peng [3,*], Zhong-Hua Huang [2], Qiao Liang [1,2], Jie Liu [1,2] and Wen-Quan Zhou [1]

[1] School of Architectural Engineering, Hunan Institute of Engineering, Xiangtan 411104, China
[2] Hunan Provincial Key Laboratory of Intelligent Disaster Prevention-Mitigation and Ecological Restoration in Civil Engineering, Xiangtan 411104, China
[3] School of Civil Engineering, Central South University, Changsha 410075, China
* Correspondence: xiaojunst@stu.csust.edu.cn (S.-N.L.); pengzhu@csu.edu.cn (Z.P.)

Abstract: Clarifying the time-dependent strength deterioration characteristics of carbonaceous mudstone under dry and wet cycles is of great significance to the design of expressway cut slopes. In this work, we conducted triaxial compression creep tests on carbonaceous mudstone specimens that had undergone different numbers of dry and wet cycles to investigate their creep properties. A function was established between the steady-state viscoplastic creep rate and axial compression. The threshold stress of the steady-state viscoplastic creep rate was assumed as the long-term strength, and the long-term strength deterioration law of carbonaceous mudstone under dry and wet cycles was studied. The results showed that the transient strain, viscoelastic creep, and viscoplastic creep of carbonaceous mudstone increased with the number of dry and wet cycles, and the creep failure stress and transient elasticity modulus decreased. Based on the steady-state viscoplastic creep rate method, the long-term strength of carbonaceous mudstone after n (n = 0, 3, 6, 9) dry and wet cycles was found to be 74.25%, 64.88%, 57.56%, and 53.16% of its uniaxial compression strength, respectively. Compared with the isochronous curve method and the transition creep method, the steady-state viscoplastic creep rate method can more accurately determine the long-term rock strength. The long-term strength of carbonaceous mudstone under dry and wet cycles decays exponentially, and the long-term strength decay rate during the first three dry and wet cycles is about 215 times the average decay rate.

Keywords: geotechnical engineering; carbonaceous mudstone; dry and wet cycles; creep; long-term strength

Citation: Li, S.-N.; Peng, Z.; Huang, Z.-H.; Liang, Q.; Liu, J.; Zhou, W.-Q. Time-Dependent Deformation and Long-Term Strength of Carbonaceous Mudstone under Dry and Wet Cycles. *Sustainability* **2022**, *14*, 12044. https://doi.org/10.3390/su141912044

Academic Editor: Anjui Li

Received: 27 July 2022
Accepted: 19 September 2022
Published: 23 September 2022

1. Introduction

At present, many slopes suffer from creep failure during operation, which is mostly caused by inaccurate calculation of the long-term strength of soft rocks under dry and wet cycles [1,2]. Correctly understanding the creep characteristics of soft rocks under dry and wet cycles and accurately evaluating their long-term strength is a challenging issue and a research focus [3–5].

The mineral composition and mesostructure of soft rocks have obvious time-dependent deterioration characteristics, and their mineral dissolution and micro-structure deterioration under dry and wet cycles also intensify the rock deformation development [6–8]. Due to the time-dependent deterioration of the rocks in the cut slopes and their long-term strength declining below the peak strength under continuous loading, some originally stable slopes undergo creeping failure during operation [9–11]. Accurately calculating the long-term strength of rocks has been a concern of scholars in geotechnical engineering [12–14]. Schmidtke et al. [15] proposed to set the minimum load for fatigue failure of rocks as their long-term strength. Szczepanik et al. [16] discriminated the long-term strength of rocks based on whether the volume of the specimen was expanded. In essence, the most direct determination of the long-term strength of rocks is to obtain the minimum creep failure stress

via creep tests, which requires a large number of creep tests and is difficult to implement in practical engineering [17,18]. Subsequently, the transition creep method was adopted to simplify the loading of the direct method and significantly reduce the experimental work, though only the range of long-term strength was determined (China GB/T50266-2013) [19]. To address this limitation, scholars proposed the isochronous curve method, i.e., drawing an isochronous curve with the creep of different stresses at a certain moment and taking the inflection point of the curve as the long-term strength of the rock, thus solving the problem that the transition creep method cannot accurately determine the long-term strength [20,21]. However, it is worth noting that some rocks lack obvious inflection points on the isochronous curve [22–24], and the applicability of the isochronous curve method still requires further investigation. Nara et al. [25] proposed to estimate the long-term strength of rocks with the subcritical crack growth information. Ding et al. [26] suggested that the inflection point at which the volumetric strain of the rock shifts from compression to expansion can be taken as the long-term strength. Wu et al. [27] consider that it is more accurate to use the inflection point of steady-state creep rate as the long-term strength of rock. In summary, despite the many methods to determine the long-term strength of rocks, their results vary, and the accurate determination of the long-term strength of soft rocks still needs in-depth studies. In addition, the mechanical properties of carbonaceous mudstone under dry and wet cycles are more complex than those of ordinary rocks [28–31]. Although scholars have conducted a lot of research on the mechanical properties, creep properties, and constitutive relations of soft rocks under dry and wet cycles [32–36], there are few studies on the evolution of the long-term strength of carbonaceous mudstone under dry and wet cycles.

Therefore, we conducted triaxial compression creep tests on carbonaceous mudstone specimens that had undergone different numbers of dry and wet cycles. On the basis of an in-depth study of the creep properties of carbonaceous mudstone, the function between the steady-state viscoplastic creep rate and stress was established. Thus, an accurate method to determine the long-term strength of carbonaceous mudstone is proposed to clarify the long-term strength evolution of carbonaceous mudstone under dry and wet cycles. The research results could provide insightful references for the design of soft rock cut slope supports.

2. Test Method

2.1. Specimen Characteristics

The carbonaceous mudstone specimens were collected from the high and steep carbonaceous mudstone slopes in Liuzhai, Guangxi, which had excavation heights between 70.0 and 80.0 m. Complete rock blocks at the foot of the slopes were collected and sealed for transportation to the indoor test site. The rock specimens were dark gray, moderately weathered, and uniformly granular with microfractures. The physical and mechanical parameters of the carbonaceous mudstone specimens are shown in Table 1.

Table 1. Physical and mechanical parameters of carbonaceous mudstone samples.

Density ($g \cdot cm^{-3}$)	Water Content (%)	Uniaxial Compressive Strength (MPa)	Elasticity Modulus (GPa)	Longitudinal Wave Velocity ($m \cdot s^{-1}$)	Water Absorption Capacity (%)	Disintegration Resistance Index I_{d2} (%)
2.36~2.43	1.24	35.65	5.32	3084~3256	9.41~14.68	85.2~90.4

2.2. Dry and Wet Cycle Test

The specimens were divided into four groups, which were subjected to n (n = 0, 3, 6, 9) dry and wet cycles. In order to simulate the extreme climatic conditions in Guangxi, the specimens were firstly dried at 50 °C in an oven for 24 h and then cooled to room temperature in a humidor before undergoing natural water absorption for 24 h in a water container. Each dry and wet cycle lasted 48 h.

2.3. Triaxial Compression Creep Test

An RLW-2000 triaxial creep tester was used to perform triaxial compression creep tests on the specimens that underwent different dry and wet cycles by using the graded incremental loading method. The maximum load of RLW-2000 triaxial creep tester is 2000 kN; the force measurement range is 2~100%, the displacement measurement range is 0~20 mm, the measurement accuracy is within ±0.5% of the indicated value, and the confining pressure measurement range is 0~50 MPa. The loaded confining pressure was 2 MPa before applying the axial pressure. The first stage of the creep test was loaded at 40% of the uniaxial compression strength, i.e., 14.26 MPa. The graded loading increments were 3 MPa, and each grade of loading stress lasted 48 h before the next grade of loading was applied, unless the specimen failed.

3. Test Results

The results of the triaxial compression creep test on carbonaceous mudstone are shown in Figure 1. The carbonaceous mudstone specimens with zero and three dry and wet cycles were in the decay creep stage at the first four loading grades (23.26 MPa). The same specimens entered the steady-state creep stage at the fifth loading grade (26.26 MPa) and the accelerated creep failure stage at the eighth loading grade, reaching a creep failure stress of 35.26 MPa. In contrast, the carbonaceous mudstone specimens with six and nine dry and wet cycles were in the decay creep stage only at the first three loading stages (14.26 MPa, 17.26 MPa, and 20.26 MPa). The same specimens entered the steady-state creep stage from the fourth loading grade (23.26 MPa) and the accelerated creep failure stage at the axial compression of 32.26 MPa. The reason is that some of the clay minerals in the carbonaceous mudstone are dissolved due to the dry and wet cycles, and the pores gradually sprout, expand, and connect, resulting in the decreased capacity of the mechanics of rock. Under the same axial compression stress, the axial strain of carbonaceous mudstone increased with the number of dry and wet cycles. This means that the stresses required for the carbonaceous mudstone to enter the steady-state creep and accelerated creep stages decrease with the number of dry and wet cycles. The reason may be that the dry and wet cycles damaged the micro-structure of the carbonaceous mudstone. With the increase in dry and wet cycles, the internal damage of the rock intensifies, resulting in increased creep and decreased creep failure stress under load.

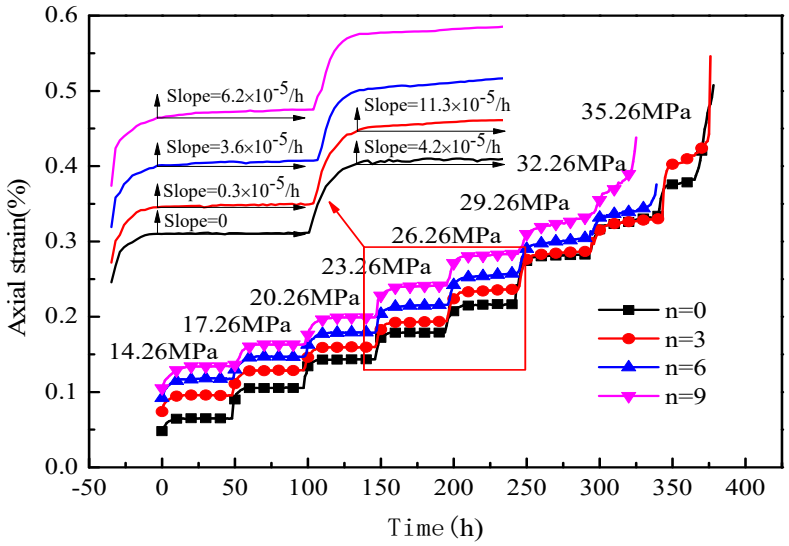

Figure 1. Triaxial compression creep curve of carbonaceous mudstone.

4. Creep Analysis

A typical graded loading creep curve of the rock is shown in Figure 2. When the axial compression stress is small, the rock undergoes transient elastic strain under stress, and the creep rate gradually decreases. After a period of creeping, the creep rate of the rock decreases to zero, and only viscoelastic deformation occurs at this stage. The rock creeping can be expressed as:

$$\varepsilon = \varepsilon_0 + \varepsilon_{ce} \tag{1}$$

When the axial compression is large, the rock first undergoes elastic strain, and then the creep rate gradually decreases to a stable non-zero value, at which stage the rock undergoes viscoelastic–plastic creep. The rock creeping can be expressed as:

$$\varepsilon = \varepsilon_0 + \varepsilon_{ce} + \varepsilon_{cp} \tag{2}$$

where ε_0, ε_{ce}, and ε_{cp} are the transient strain, viscoelastic creep, and viscoplastic creep, respectively.

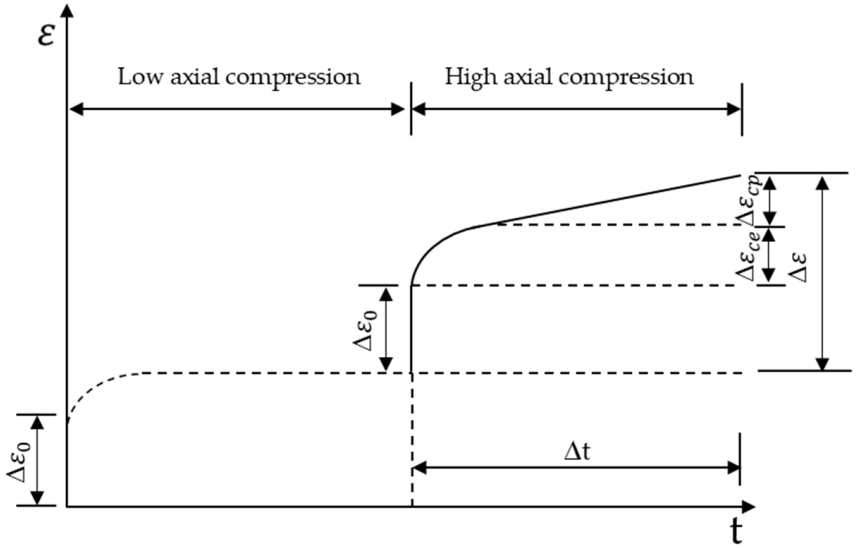

Figure 2. Typical graded load creep curve of rocks.

Zhao et al. [37] suggested that the creep properties of rocks can be studied by separating the viscoelastic and viscoplastic creep. According to the element theory, the viscoelastic creep of rocks is a stress-dependent function. By establishing a function of viscoelastic creep of the rock and stress under low axial compression and substituting it into Equation (2), the viscoplastic creep of the rock at high axial compression can be separated.

4.1. Transient Strain

The transient strains of carbonaceous mudstone under different dry and wet cycles are shown in Figure 3. The transient strains of carbonaceous mudstone under the same dry and wet cycles increased with axial compression stress σ_c. For example, with six dry and wet cycles, the transient strain under the axial compression stress of 20.26 MPa and 29.26 MPa was 93.3% and 185.9% larger than that under the axial compression stress of 14.26 MPa, respectively. Under the same axial compression stress, the transient strain of carbonaceous mudstone increased with the number of dry and wet cycles. For instance, under the axial compression of 20.26 MPa, the transient strain of carbonaceous mudstone with three, six, and nine dry and wet cycles was 8.26%, 22.31%, and 35.54% larger than that with zero cycles, respectively. The reason may be the dissolution of hydrophilic minerals of carbonaceous mudstone under dry and wet cycles, which promoted the development and

expansion of its microfractures and microporosity [38,39]. As a result, the effective bearing area of the rock decreases, and a large transient strain is generated under the load.

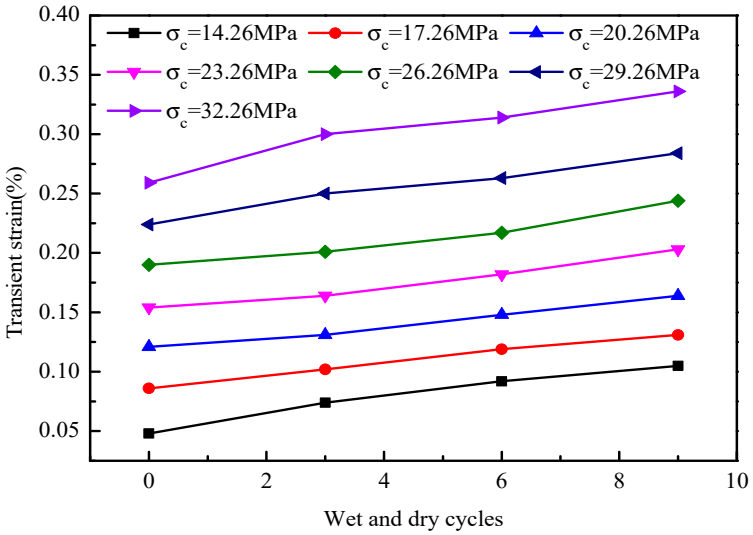

Figure 3. The transient strain of carbonaceous mudstone.

4.2. Viscoelastic Creep Analysis

The viscoelastic creep of carbonaceous mudstone calculated from Equation (1) is shown in Figure 4. The viscoelastic creep of the rock increased with time, but the creep rate gradually decreased and stabilized. With the number of dry and wet cycles, the viscoelastic creep of carbonaceous mudstone increased. The viscoelastic creep of carbonaceous mudstone with zero, three, six, and nine dry and wet cycles was 2.2×10^{-4}, 2.6×10^{-4}, 3.1×10^{-4}, and 3.5×10^{-4}, respectively. Compared to the carbonaceous mudstone with no dry and wet cycles, the viscoelastic creep of that with three, six, and nine dry and wet cycles was 18.18%, 40.91%, and 59.09% larger, respectively. The viscoelastic creep of rocks can be described by the well-established element theory and empirical models [1]. In this paper, the Kelvin model is used to fit the viscoelastic creep, which is expressed as Equation (3). The fitted parameters are shown in Table 2.

$$\varepsilon_{ce} = \varepsilon_{ce}^{\infty}[1 - \exp(-\frac{E_{ce}}{\eta_{ce}}t)] \tag{3}$$

As shown in Table 2, $\varepsilon_{ce}^{\infty}$ and $\frac{E_{ce}}{\eta_{ce}}$ in the viscoelastic creep model of carbonaceous mudstone with different numbers of dry and wet cycles are stress-related parameters. Fitting via the least square method yields the function of viscoelastic creep model parameters as:

$$\varepsilon_{ce}^{\infty} = a\sigma_c + b \cdot \exp(c\sigma_c) \tag{4}$$

$$\frac{E_{ce}}{\eta_{ce}} = d\sigma_c + e \tag{5}$$

where a, b, c, d, and e are the parameters related to the number of dry and wet cycles, and their values are shown in Table 3.

The viscoelastic creep of the rock at high axial compression can be obtained by substituting the grade 5 to grade 8 axial compression into Equation (3), as shown in Figure 5. It can be seen that the viscoelastic creep changes at the high and low axial compression are similar. The viscoelastic creep increases with the axial compression and the number of dry and wet cycles, while the creep rate gradually decreases and finally stabilizes.

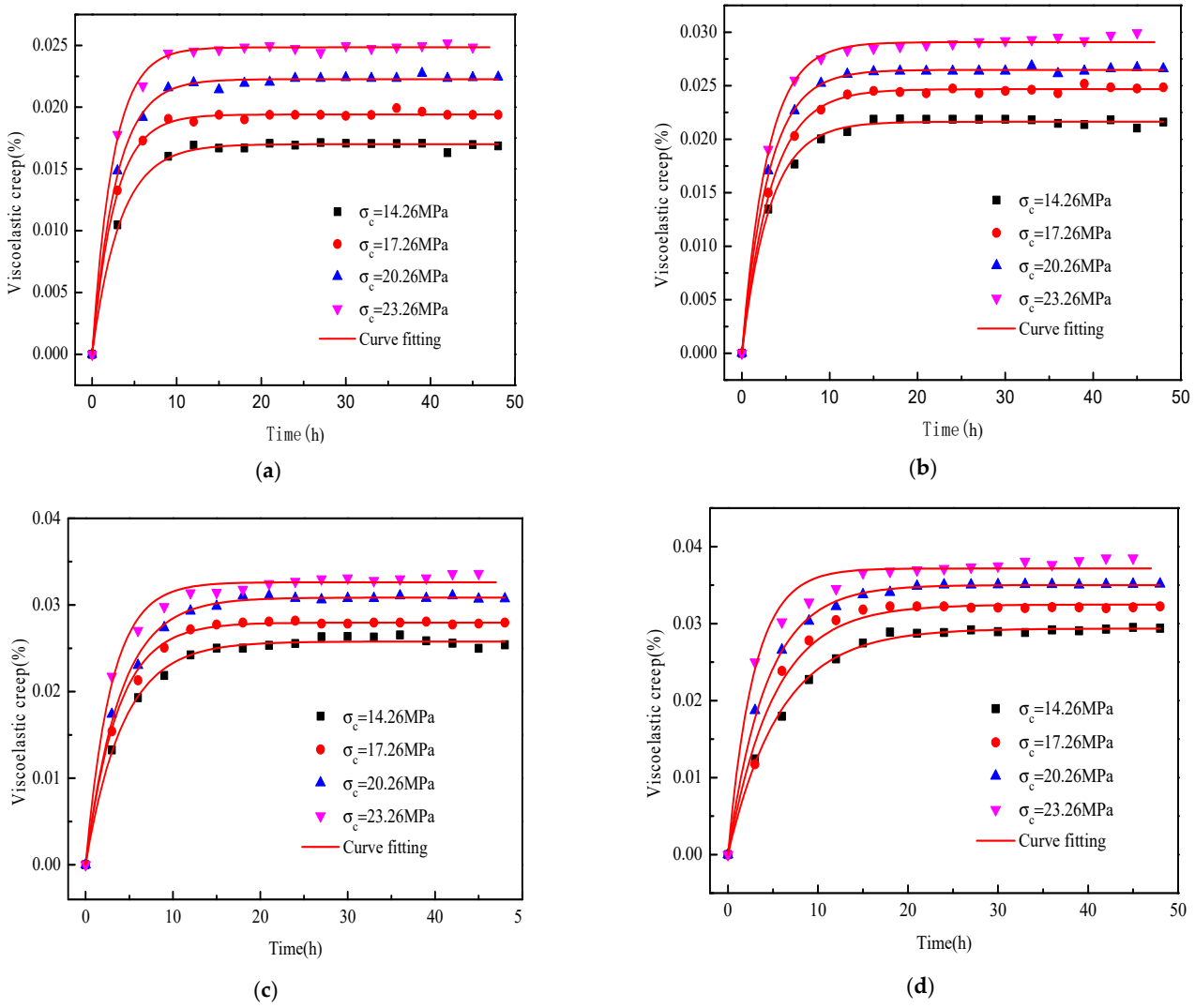

Figure 4. Viscoelastic creep of carbonaceous mudstone under low axial compression. (**a**) No dry and wet cycle, (**b**) 3 dry and wet cycles, (**c**) 6 dry and wet cycles, (**d**) 9 dry and wet cycles.

Table 2. Viscoelastic creep fitting parameters of carbonaceous mudstone.

Axial Compression/MPa	0 Dry and Wet Cycle		3 Dry and Wet Cycles		6 Dry and Wet Cycles		9 Dry and Wet Cycles	
	$\varepsilon_{ce}^{\infty}$ (10^{-4})	$\frac{E_{ce}}{\eta_{ce}}$	$\varepsilon_{ce}^{\infty}$ (10^{-4})	$\frac{E_{ce}}{\eta_{ce}}$	$\varepsilon_{ce}^{\infty}$ (10^{-4})	$\frac{E_{ce}}{\eta_{ce}}$	$\varepsilon_{ce}^{\infty}$ (10^{-4})	$\frac{E_{ce}}{\eta_{ce}}$
14.26	1.700	0.2991	2.164	0.3145	2.577	0.2341	2.936	0.1718
17.26	1.941	0.3728	2.467	0.2992	2.796	0.2749	3.247	0.1967
20.26	2.226	0.3518	2.648	0.3306	3.085	0.2554	3.502	0.2346
23.26	2.473	0.4105	2.900	0.3499	3.256	0.3444	3.711	0.3501

Table 3. Dry and wet cycles parameters of carbonaceous mudstone.

Dry and Wet Cycles	a (10^{-4})	b (10^{-4})	c	d	e
0	7.210	50.128	2.013×10^{-9}	0.0104	0.1626
3	7.963	105.083	1.051×10^{-9}	0.0046	0.2375
6	7.753	147.397	2.796×10^{-10}	0.0103	0.0825
9	8.560	173.563	2.680×10^{-10}	0.0191	−0.1198

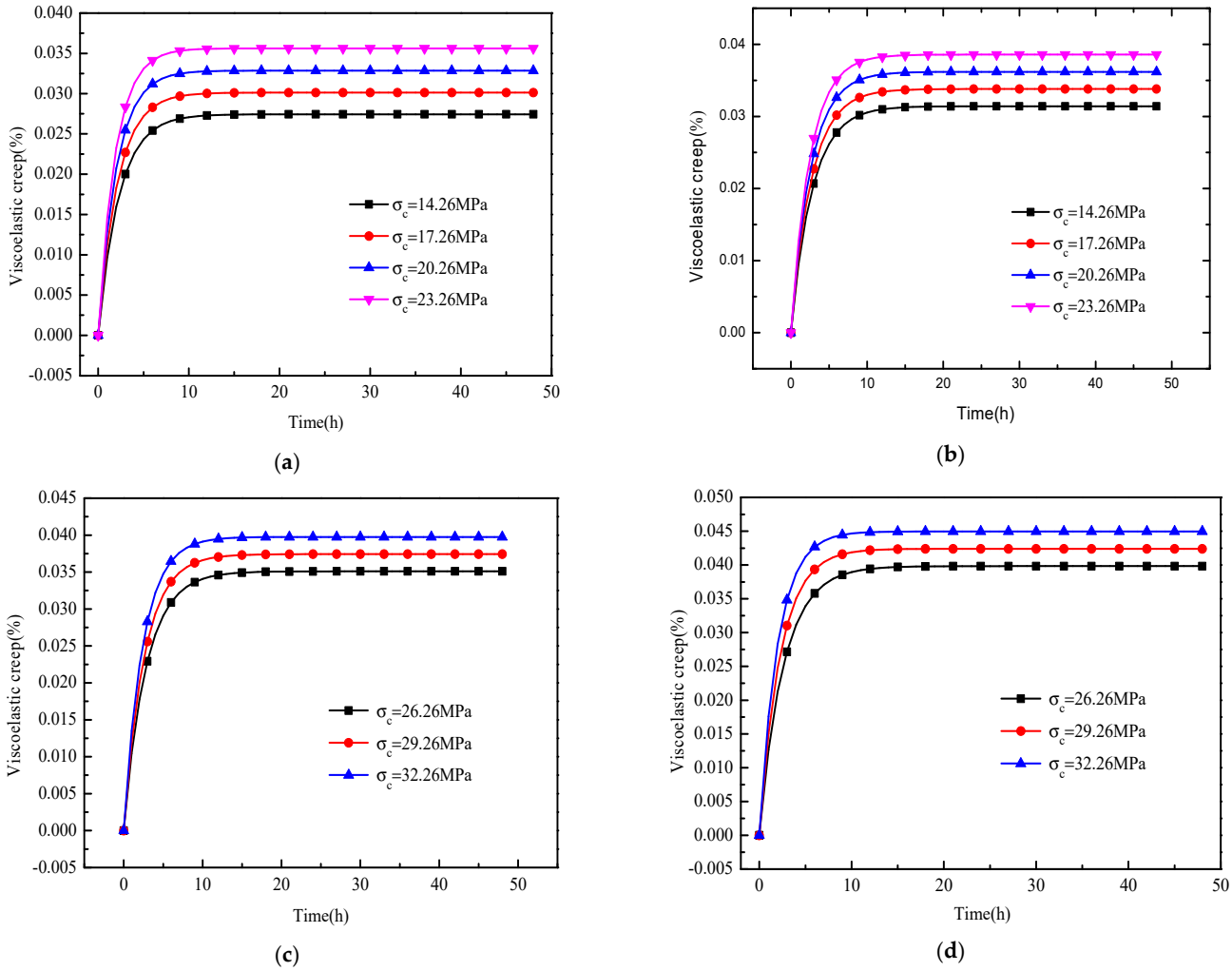

Figure 5. Viscoelastic creep of carbonaceous mudstone under high axial compression. (**a**) No dry and wet cycle, (**b**) 3 dry and wet cycles, (**c**) 6 dry and wet cycles, (**d**) 9 dry and wet cycles.

4.3. Viscoplastic Creep Analysis

The viscoplastic creep can be separated from the total strain by substituting the calculated viscoelastic creep into Equation (2). The viscoplastic creep of carbonaceous mudstone under different dry and wet cycles is shown in Figure 6. The viscoplastic creep of carbonaceous mudstone increased with the number of dry and wet cycles. For example, under an axial compression of 29.26 MPa for 20 h, the viscoplastic creep of carbonaceous mudstone with n (n = 0, 3, 6, 9) dry and wet cycles was 3.0×10^{-4}, 1.0×10^{-4}, 1.1×10^{-4}, and 2.0×10^{-4}, respectively, averaging a 1.89×10^{-5} increase for each cycle. When the stress was below the failure stress, the viscoplastic creep was at the decay creep stage first before maintaining a steady rate of growth. However, when the stress exceeded the creep failure threshold stress, the viscoplastic creep of carbonaceous mudstone accelerated. It is worth noting that the stress required for the carbonaceous mudstone to enter the accelerated viscoplastic creep stage decreased with the number of dry and wet cycles. With zero and three dry and wet cycles, the carbonaceous mudstone entered the accelerated viscoplastic creep stage at the axial compression stress of 35.26 MPa. However, the carbonaceous mudstone with six and nine dry and wet cycles entered the accelerated viscoplastic creep stage at the axial compression stress of 32.26 MPa.

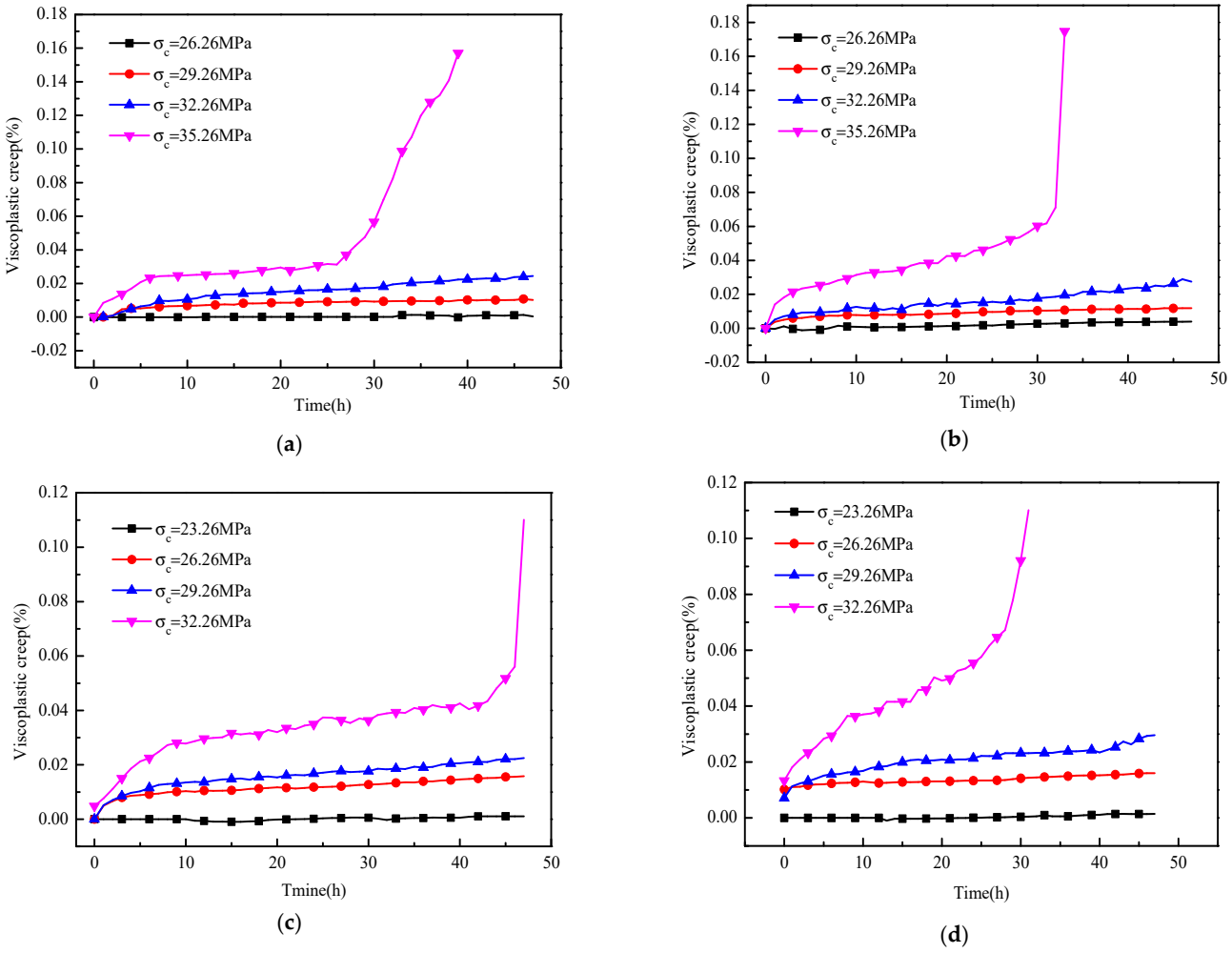

Figure 6. Viscoplastic creep of carbonaceous mudstone. (**a**) No dry and wet cycle, (**b**) 3 dry and wet cycles, (**c**) 6 dry and wet cycles, (**d**) 9 dry and wet cycles.

5. Long-Term Strength Analysis

5.1. The Steady-State Viscoplastic Creep Method

Viscoelastic and viscoplastic creep analyses of carbonaceous mudstone reveal that at lower axial compression, only viscoelastic creep occurs or the creep rate decreases to zero after a short period of viscoplastic deformation, and the rock could remain stable. As the stress exceeds the threshold stress of steady-state viscoplastic creep, the steady-state viscoplastic creep or accelerated creep shows growth, and the rock eventually undergoes deformation failure with the accumulation of viscoplastic creep. It can be seen that the threshold stress of steady-state viscoplastic creep of the rock is its long-term strength. Thus, the function of steady-state viscoplastic creep rate and stress can be established to determine the long-term strength of the rock. The steady-state viscoplastic creep rates of carbonaceous mudstone were obtained by linearly fitting the steady-state viscoplastic creep stages in Figure 6, as shown in Table 4.

Table 4. Steady-state viscoplastic creep rate (10^{-8}/h).

Axial Compression (MPa)	Dry and Wet Cycles			
	0	**3**	**6**	**9**
23.26	0	0	0.36	0.62
26.26	0.03	1.10	1.62	1.72
29.26	0.74	1.26	2.42	4.10
32.26	3.55	5.85	4.70	11.72
35.26	3.93	12.74	/	/

The relationship between the steady-state viscoplastic creep rate and axial compression is shown in Figure 7. It can be seen that the steady-state viscoplastic creep increases exponentially with axial compression, and its functional relationship is as follows:

$$\dot{\varepsilon}_{cp} = A \cdot \exp(B \cdot \sigma_c) + C \quad (6)$$

where $\dot{\varepsilon}_{cp}$ is the steady-state viscoplastic creep rate, and A, B, and C are the fitting parameters.

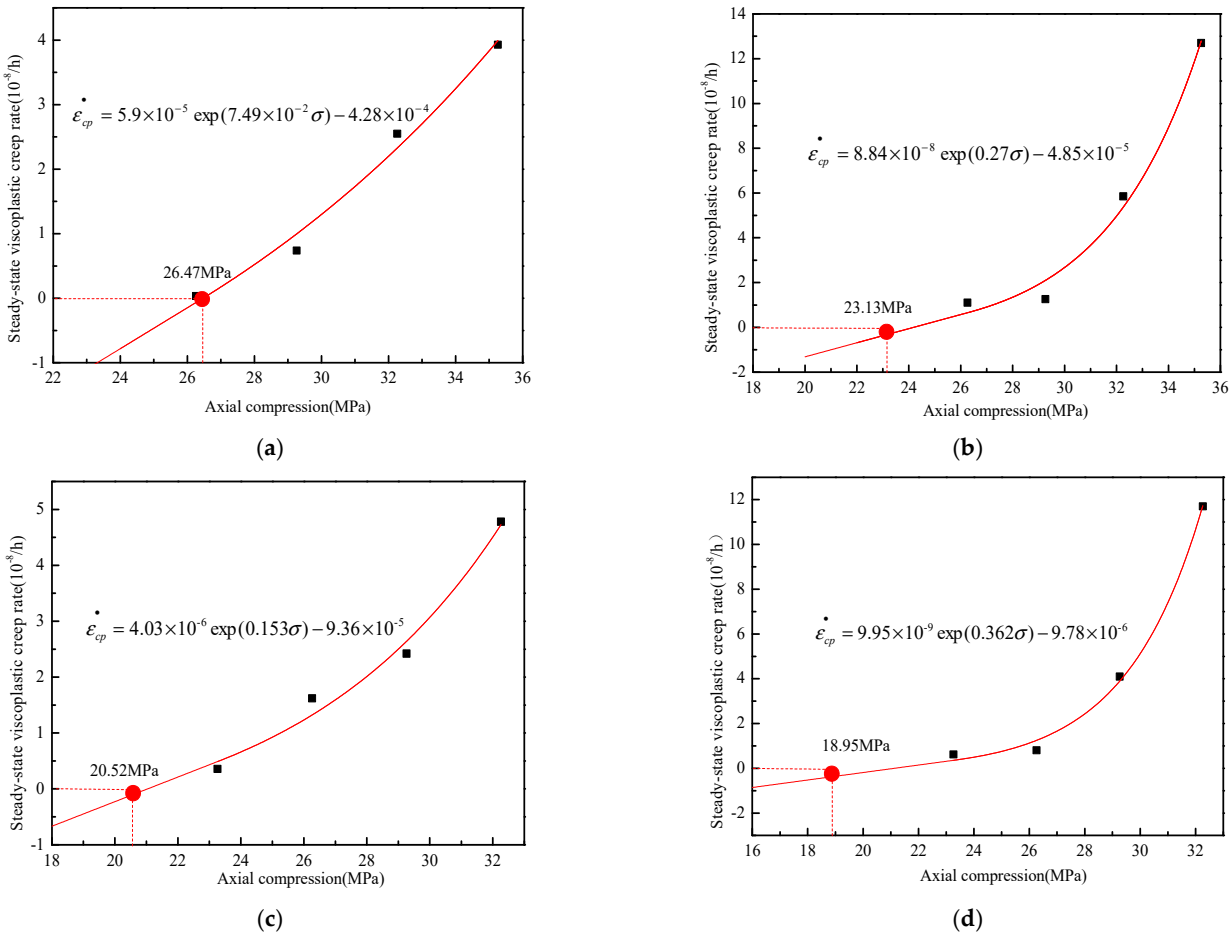

Figure 7. The relationship between steady-state viscoplastic creep rate and axial compression of carbonaceous mudstone. (**a**) No dry and wet cycle, (**b**) 3 dry and wet cycles, (**c**) 6 dry and wet cycles, (**d**) 9 dry and wet cycles.

Based on Equation (6), the threshold stress at which the steady-state viscoplastic creep rate is zero is the long-term strength of the rock. The long-term strength of carbonaceous mudstone after zero, three, six, and nine dry and wet cycles was 26.47 MPa, 23.13 MPa,

20.52 MPa, and 18.95 MPa, which was 74.25%, 64.88%, 57.56%, and 53.16% of its uni-axial compression strength, respectively.

5.2. The Isochronous Curve Method

With the isochronous curve method, the strain under different loading stresses at the same time is plotted as an isochronous line, and the inflection point of the isochronous curve cluster is assumed as the long-term strength of the rock. The creep isochronous curve clusters of carbonaceous mudstone under different numbers of dry and wet cycles are shown in Figure 8. The isochronous curve clusters of carbonaceous mudstone become progressively sparse with the number of dry and wet cycles. Under the same number of dry and wet cycles, the density of isochronous curve clusters of carbonaceous mudstone decreases with axial compression, and the curves gradually deviate to the strain axis. However, according to the experimental results in Figure 8, it is difficult to accurately find the inflection point of the isochronous curve. The long-term strengths of carbonaceous mudstone with zero, three, six, and nine dry and wet cycles were subjectively determined as 32.26 MPa, 29.26 MPa, 26.26 MPa, and 26.26 MPa, respectively, based on the pattern of the isochronous curve.

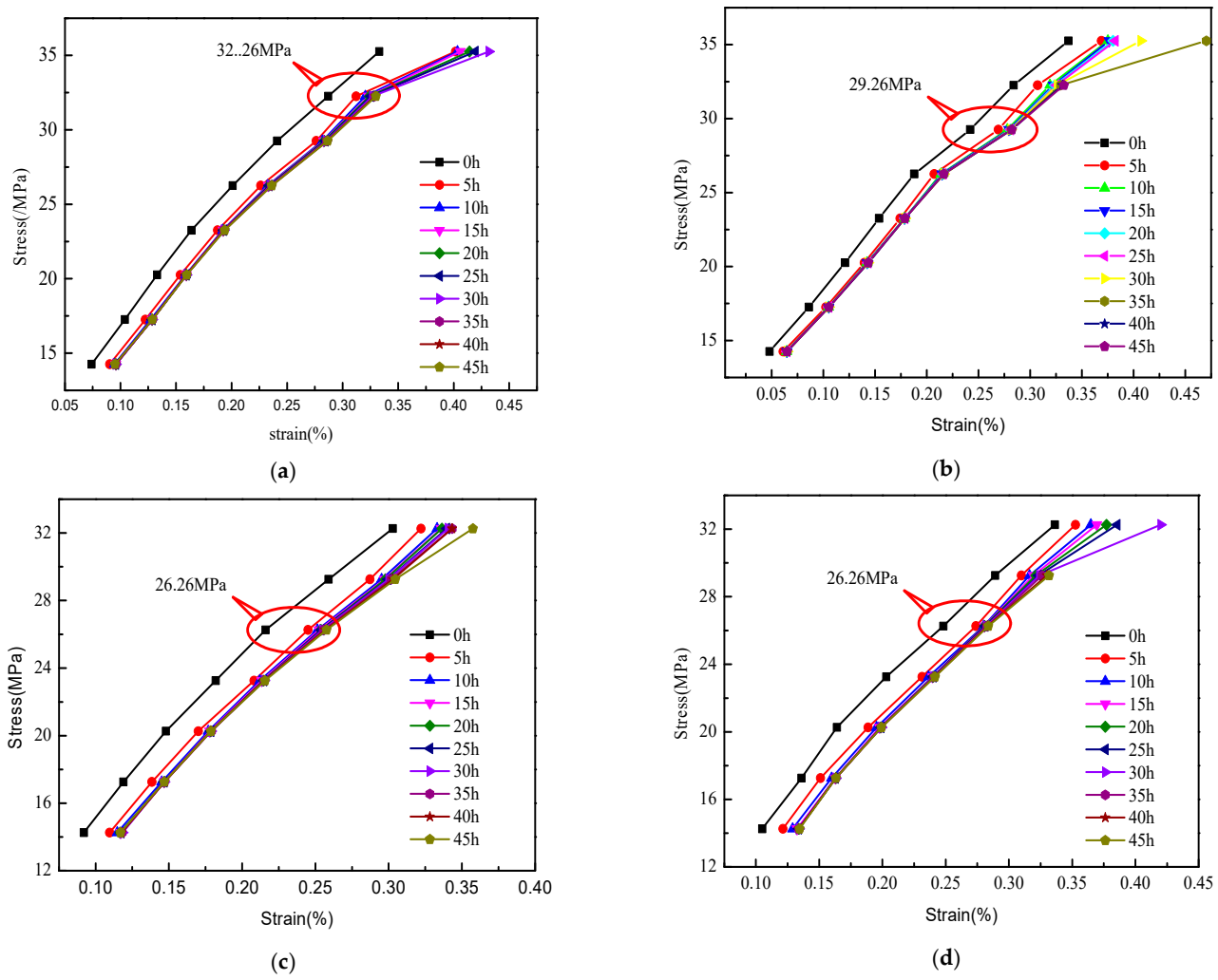

Figure 8. Isochronous curve clusters of carbonaceous mudstone. (**a**) No dry and wet cycle, (**b**) 3 dry and wet cycles, (**c**) 6 dry and wet cycles, (**d**) 9 dry and wet cycles.

5.3. The Transition Creep Method

The transition creep method considers the maximum load stress at which the steady-state creep rate is zero to be the long-term strength of the rock. The viscoelastic and viscoplastic creep of carbonaceous mudstone were fitted using $\varepsilon_{ce} = A[B - \exp(Ct)]$ and $\varepsilon_{cp} = Dt$, respectively, according to the results in [11]. The creep curves of carbonaceous mudstone with different dry and wet cycles at the various load grades are shown in Figure 9, and the corresponding fitting functions are shown in Table 5. According to Table 5, the transition creep method can only determine the long-term strength range of the rocks, and the long-term strength ranges of carbonaceous mudstone with zero, three, six, and nine dry and wet cycles are 26.26 to 29.26 MPa, 23.26 to 26.26 MPa, 20.26 to 23.26 MPa, and 17.26 to 20.26 MPa, respectively.

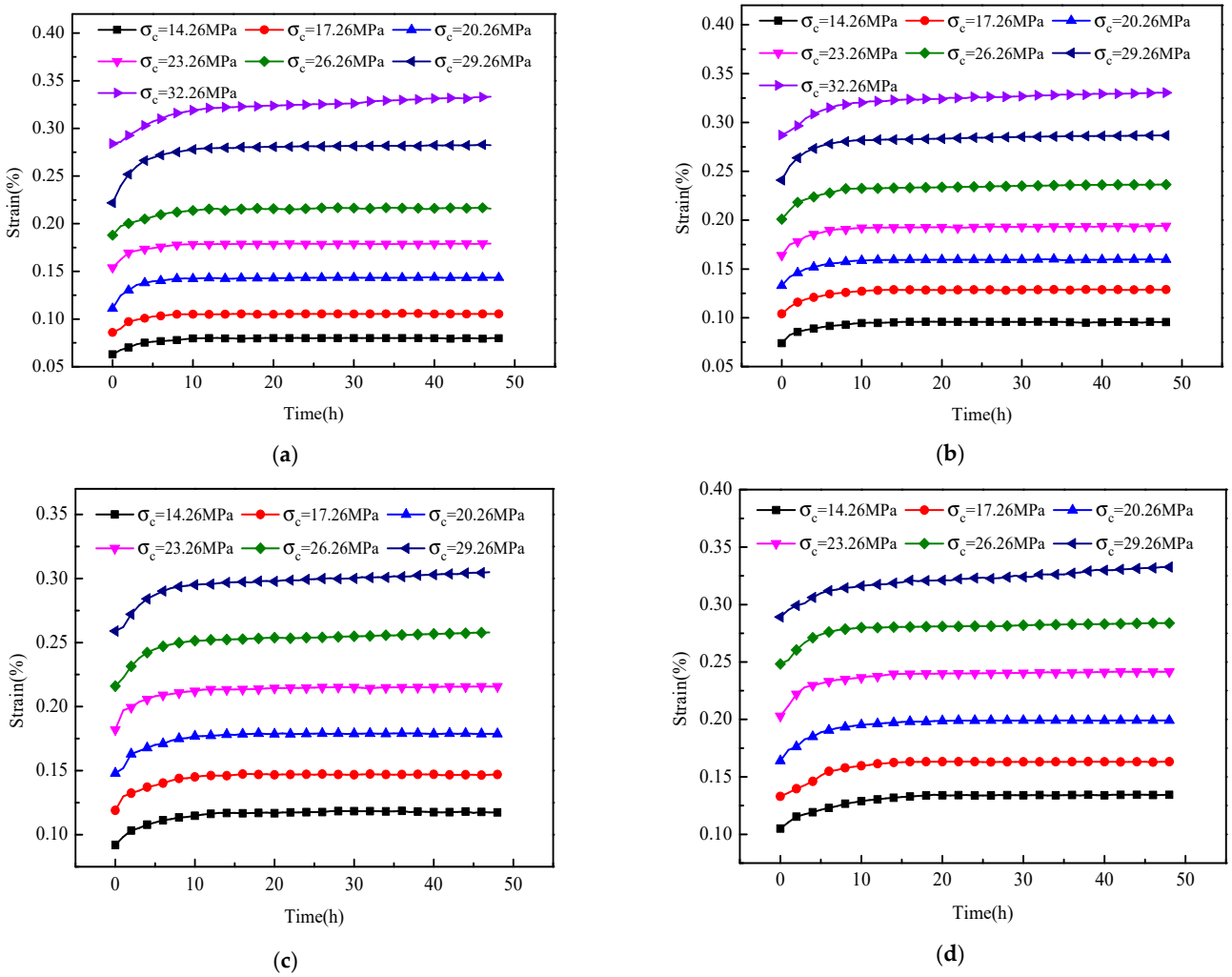

Figure 9. The creep curve of carbonaceous mudstone under various loadings. (**a**) No dry and wet cycle, (**b**) 3 dry and wet cycles, (**c**) 6 dry and wet cycles, (**d**) 9 dry and wet cycles.

Table 5. The fitting function of creep curve of carbonaceous mudstone under various loadings.

0 Dry and Wet Cycles		3 Dry and Wet Cycles	
Axial Compression (MPa)	**Fitting Function**	**Axial Compression (MPa)**	**Fitting Function**
14.26	$\varepsilon = 0.017[3.828 - \exp(-0.30t)]$	14.26	$\varepsilon = 0.020[4.756 - \exp(-0.289t)]$
17.26	$\varepsilon = 0.020[5.250 - \exp(-0.385t)]$	17.26	$\varepsilon = 0.024[5.326 - \exp(-0.292t)]$
20.26	$\varepsilon = 0.023[6.218 - \exp(-0.364t)]$	20.26	$\varepsilon = 0.026[6.196 - \exp(-0.321t)]$
23.26	$\varepsilon = 0.024[7.317 - \exp(-0.397t)]$	23.26	$\varepsilon = 0.028[6.884 - \exp(-0.333t)]$
26.26	$\varepsilon = 0.027[8.120 - \exp(-0.236t)]$	26.26	$\varepsilon = 0.031[7.553 - \exp(-0.350t)] + 1.02 \times 10^{-4}t$
29.26	$\varepsilon = 0.044[6.415 - \exp(-0.248t)] + 3.37 \times 10^{-5}t$	29.26	$\varepsilon = 0.040[7.071 - \exp(-0.404t)] + 1.26 \times 10^{-4}t$
32.26	$\varepsilon = 0.040[7.990 - \exp(-0.214t)] + 2.847 \times 10^{-4}t$	32.26	$\varepsilon = 0.032[10.168 - \exp(-0.233t)] + 1.96 \times 10^{-4}t$
6 Dry and Wet Cycles		**9 Dry and Wet Cycles**	
Axial Compression (MPa)	**Fitting Function**	**Axial Compression (MPa)**	**Fitting Function**
14.26	$\varepsilon = 0.025[4.741 - \exp(-0.224t)]$	14.26	$\varepsilon = 0.029[4.685 - \exp(-0.167t)]$
17.26	$\varepsilon = 0.026[5.666 - \exp(-0.253t)]$	17.26	$\varepsilon = 0.032[5.170 - \exp(-0.193t)]$
20.26	$\varepsilon = 0.031[5.717 - \exp(-0.259t)]$	20.26	$\varepsilon = 0.034[5.844 - \exp(-0.234t)] + 1.383 \times 10^{-5}t$
23.26	$\varepsilon = 0.028[7.056 - \exp(-0.381t)] + 7.434 \times 10^{-5}t$	23.26	$\varepsilon = 0.030[7.770 - \exp(-0.410t)] + 8.399 \times 10^{-5}t$
26.26	$\varepsilon = 0.036[6.893 - \exp(-0.331t)] + 1.452 \times 10^{-4}t$	26.26	$\varepsilon = 0.034[8.219 - \exp(-0.322t)] + 1.123 \times 10^{-4}t$
29.26	$\varepsilon = 0.038[7.662 - \exp(-0.299t)] + 2.118 \times 10^{-4}t$	29.26	$\varepsilon = 0.028[11.474 - \exp(-0.261t)] + 3.85 \times 10^{-4}t$

5.4. Analysis and Discussion

A summary of the long-term strength of carbonaceous mudstone under different dry and wet cycles obtained by the above three methods is shown in Table 6. The comparison of the three methods for solving the long-term strength of rocks showed that the inflection point of the isochronous curve method is not clear, and determining the long-term strength of rocks by subjective estimation inevitably leads to errors. The transition creep method only determines the long-term strength range of rocks and does not accurately determine the specific value of the long-term strength. The steady-state viscoplastic creep rate method proposed in this paper can accurately determine the long-term strength of rocks by establishing a function between the steady-state viscoplastic creep rate and stress. In addition, the calculated long-term strength is within the range determined by the transition creep method, indicating the feasibility of the proposed method. Therefore, the steady-state viscoplastic creep rate method can serve as a method to determine the long-term strength of rocks.

Table 6. A summary of long-term rock strength determination by different methods.

Dry and Wet Cycles	Long-Term Strength (MPa)		
	Steady-State Viscoplastic Creep Rate Method	**Isochronous Curve Method**	**Transition Creep Method**
0	26.47	32.26	26.26~29.26
3	23.13	29.26	23.26~26.26
6	20.52	26.26	20.26~23.26
9	18.95	26.26	17.26~20.26

Under continuous load, the strain of rock increases with time, and the increased strain is essentially the viscoplastic strain. Once the viscoplastic strain starts to increase rapidly, the rock will undergo creep failure after a period of strain accumulation. Therefore, it is correct and feasible to use the steady-state viscoplastic creep method to determine the long-term strength of rock. The isochronous curve method takes the stress when the strain changes abruptly as the long-term strength of the rock. In fact, this method also indirectly determines the stress point when the viscoplastic strain changes abruptly, but for some brittle rocks, the viscoplastic strain is much smaller than the elastic strain during the creep process, and the growth of the viscoplastic strain has no obvious influence on creep, so it is difficult to accurately find the inflection point of the isochronous curve. The transition creep method uses the function to fit the creep curve, and also indirectly determines the stress of the accelerated development of rock viscoplastic strain. This method is limited by the graded loading of the creep test, and can only determine the approximate range of long-term strength.

6. The Effects of Dry and Wet Cycles on Long-Term Strength

The long-term strength of carbonaceous mudstone under dry and wet cycles determined using the steady-state viscoplastic creep rate method is shown in Figure 10. The long-term strength of carbonaceous mudstone decays exponentially with the number of dry and wet cycles, which can be fitted as:

$$\sigma_\infty = -3.021 \ln(1 + n) + 26.78 \quad (7)$$

where σ_∞ is the long-term strength, and n is the number of dry and wet cycles.

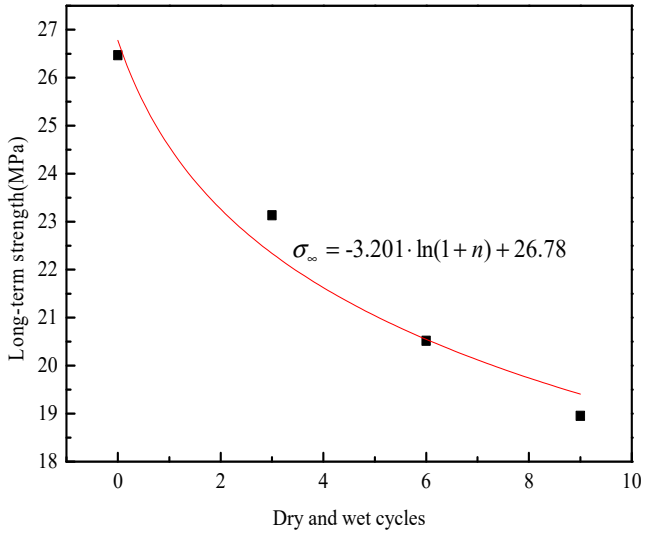

Figure 10. The long-term strength of carbonaceous mudstone under dry and wet cycles.

The long-term strength of carbonaceous mudstone decays to zero after 5113 dry and wet cycles. The average long-term strength average decay rate of carbonaceous mudstone under dry and wet cycles is about 0.005 MPa/cycle. The long-term strength decay rate during the first three dry and wet cycles is 1.113 MPa/cycle. Thus, the long-term strength decay rate of the first three dry and wet cycles is about 215 times the average decay rate. The reason may be the rock structure damage and deterioration caused by the mineral dissolution and crack expansion of carbonaceous mudstone under dry and wet cycles. As the dry and wet cycle continues, the soluble minerals on the rock surface are gradually dissolved, and the chance of water contacting them decreases. In the meantime, with the crack expansion, the crack expansion energy is gradually released at the crack end, and the kinetic energy of the crack expansion decreases. These are the reasons leading to a decrease in the deterioration rate of the long-term strength of carbonaceous mudstone.

7. Conclusions

We studied the time-dependent deformation and long-term strength of carbonaceous mudstone under dry and wet cycles, and the following conclusions can be drawn.

(1) The transient strain, viscoelastic creep, and viscoplastic creep of carbonaceous mudstone increased with the number of dry and wet cycles, and the creep failure stress decreased. Therefore, the dry and wet cycles intensified the development of creep in carbonaceous mudstone and accelerated the creep failure of the rock.

(2) Determining the long-term strength of carbonaceous mudstone with the threshold stress of steady-state viscoplastic creep rate was more advantageous than using the isochronous curve method and the transition creep method, thus providing a new method for studying the long-term strength of soft rocks.

(3) The long-term strength of carbonaceous mudstone decays exponentially with the number of dry and wet cycles, and the long-term strength decay rate during the first

three dry and wet cycles is about 215 times the average decay rate. Therefore, the cut slopes with carbonaceous mudstone should be waterproofed in time after excavation.

Author Contributions: Conceptualization, S.-N.L.; methodology, S.-N.L.; validation, Z.P. and Q.L.; formal analysis, Z.P.; investigation, Z.-H.H.; resources, J.L.; data curation, Z.P.; writing—original draft preparation, S.-N.L.; writing—review and editing, W.-Q.Z.; visualization, J.L.; supervision, S.-N.L.; funding acquisition, S.-N.L. and Q.L. All authors have read and agreed to the published version of the manuscript.

Funding: This research was funded by the National Natural Science Foundation of China (52108405), the Hunan Provincial Natural Science Foundation Project (2022JJ40122), and the Scientific Research Foundation of Hunan Provincial Education Department (20A118, 21A0453, 21A0462, 21B0659).

Data Availability Statement: The data used to support the results of this study are available from the corresponding authors upon request.

Acknowledgments: This research was supported by the Hunan Provincial Key Laboratory of Intelligent Disaster Prevention-Mitigation and Ecological Restoration in Civil Engineering, Key Investigation and Application of Intelligent Disaster Prevention-Mitigation and Ecological Restoration in Civil Engineering.

Conflicts of Interest: The authors declare no conflict of interest.

Abbreviations

ε_0	Transient strain
ε_{ce}	Viscoelastic creep
ε_{cp}	Viscoplastic creep
ε	Axial strain
$\dot{\varepsilon}_{cp}$	Steady-state viscoplastic creep rate
A	Fitting parameter
B	Fitting parameter
C	Fitting parameter
σ_∞	Long-term strength
n	Number of dry and wet cycles

References

1. Zhao, Y.L.; Wang, Y.X.; Wang, W.J.; Wan, W.; Tang, J.Z. Modeling of non-linear rheological behavior of hard rock using triaxial rheological experiment. *Int. J. Rock Mech. Min. Sci.* **2017**, *93*, 66–75. [CrossRef]
2. Sharma, K.; Kiyota, T.; Kyokawa, H. Effect of slaking on direct shear behaviour of crushed mudstones. *Soils Found.* **2017**, *57*, 288–300. [CrossRef]
3. Ishizawa, T.; Danjo, T.; Sakai, N. Real-Time Prediction Method for Slope Failure Caused by Rainfall Using Slope Monitoring Records. *J. Disaster Res.* **2017**, *12*, 980–992. [CrossRef]
4. Deng, H.F.; Zhou, M.L.; Li, J.L.; Sun, X.S.; Huang, Y.L. Creep degradation mechanism by water-rock interaction in the red-layer soft rock. *Arab. J. Geosci.* **2016**, *9*, 1–12. [CrossRef]
5. Zhao, Y.L.; Zhang, L.Y.; Wang, W.J.; Wan, W.; Li, S.Q.; Ma, W.H.; Wang, Y.X. Creep behavior of intact and cracked limestone under multi-level loading and unloading cycles. *Rock Mech. Rock Eng.* **2017**, *50*, 1409–1424. [CrossRef]
6. Liu, Z.; Zhou, C.Y.; Li, B.T.; Lu, Y.Q.; Yang, X. A dissolution-diffusion sliding model for soft rock grains with hydro-mechanical effect. *J. Rock Mech. Geotech. Eng.* **2018**, *10*, 457–467. [CrossRef]
7. Qin, Z.; Fu, H.; Chen, X. A study on altered granite meso-damage mechanisms due to water invasion-water loss cycles. *Environ. Earth Sci.* **2019**, *78*, 1–10. [CrossRef]
8. Wang, X.; Lian, B.; Feng, W. A nonlinear creep damage model considering the effect of dry-wet cycles of rocks on reservoir bank slopes. *Water* **2020**, *12*, 2396. [CrossRef]
9. Damjanac, B.; Fairhurst, C. Evidence for a long-term strength threshold in crystalline rock. *Rock Mech. Rock Eng.* **2010**, *43*, 513–531. [CrossRef]
10. Zha, E.; Zhang, Z.; Zhang, R.; Wu, S.; Li, C.; Ren, L.; Zhou, J. Long-term mechanical and acoustic emission characteristics of creep in deeply buried jinping marble considering excavation disturbance. *Int. J. Rock Mech. Min. Sci.* **2021**, *139*, 104603. [CrossRef]
11. Wu, L.Z.; Li, B.; Huang, R.Q.; Sun, P. Experimental study and modeling of shear rheology in sandstone with non-persistent joints. *Eng. Geol.* **2017**, *222*, 201–211. [CrossRef]

12. Nara, Y.; Takada, M.; Mori, D.; Owada, H.; Yoneda, T.; Kaneko, K. Subcritical crack growth and long-term strength in rock and cementitious material. *Int. J. Fract.* **2010**, *164*, 57–71. [CrossRef]
13. Yang, X.; Wang, J.; Zhu, C.; He, M. Effect of water on long-term strength of column rocks based on creep behavior in Yungang Grottoes, China. *Geotech. Geol. Eng.* **2019**, *37*, 173–183. [CrossRef]
14. González Sánchez, J.A.; Bilyy, O.L.; Yukhym, R.Y. Evaluation of the Strength of Limestone After Long-Term Weathering Under Natural Conditions. *Mater. Sci.* **2018**, *53*, 560–568. [CrossRef]
15. Schmidtke, R.H.; Lajtai, E.Z. The long-term strength of Lac du Bonnet granite. *Int. J. Rock Mech. Min. Sci. Geomech. Abstr.* **1985**, *22*, 461–465. [CrossRef]
16. Szczepanik, Z.; Milne, D.; Kostakis, K.; Eberhardt, E. Long term laboratory strength tests in hard rock. In Proceedings of the 10th ISRM Congress, Sandton, South Africa, 8–12 September 2003.
17. Shen, M.R.; Chen, H.J. Testing study of long-term strength characteristics of red sandstone. *Rock Soil Mech.* **2011**, *32*, 3301–3305.
18. Zhang, Q.Y.; Yang, W.D.; Chen, F.; Li, W.G.; Wang, J.H. Long-term strength and microscopic failure mechanism of hard brittle rocks. *Chin. J. Geotech. Eng.* **2011**, *33*, 1910–1918.
19. *GB/T50266-2013*; National Standards Compilation Group of People's Republic of China. Standard for Tests Method of Engineering Rock Masses. China Plan Press: Beijing, China, 2013.
20. Zhao, M.L.; Zhang, Q.Y. The application of cubic spline interpolation function in determining rock rheological long-term strength. *Appl. Mech. Mater.* **2014**, *580*, 205–208. [CrossRef]
21. Liu, J.F.; Lu, W.; Peng, J.L.; Lu, Z.; Yu, B. Experimental study on creep deformation and long-term strength of unloading-fractured marble. *Eur. J. Environ. Civ. Eng.* **2015**, *19*, 97–107.
22. Liu, L.; Xu, W. Experimental researches on long-term strength of granite gneiss. *Adv. Mater. Sci. Eng.* **2015**, *2015*, 187616. [CrossRef]
23. Wu, F.; Zhang, H.; Zou, Q.; Li, C.; Chen, J.; Gao, R. Viscoelastic-plastic damage creep model for salt rock based on fractional derivative theory. *Mech. Mater.* **2020**, *150*, 103600. [CrossRef]
24. Hou, R.; Shi, Y.; Xu, L.; Fu, J.; Zhang, K. Evaluating long-term strength and time to failure of sandstone with different initial damage. *Adv. Civ. Eng.* **2020**, *2020*, 7149148. [CrossRef]
25. Nara, Y.; Oe, Y.; Murata, S.; Ishida, T.; Kaneko, K. Estimation of Long-Term Strength of Rock Based on Subcritical Crack Growth. *Eng. Geol. Soc. Territ.* **2015**, *2*, 2157–2160.
26. Ding, G.S.; Liu, J.F.; Wang, L.; Zhou, Z.W. Discussion on Determination Method of Long-Term Strength of Rock Salt. *Energies* **2020**, *13*, 2460. [CrossRef]
27. Wu, F.; Gao, R.; Zou, Q.; Chen, J.; Liu, W.; Peng, K. Long-term strength determination and nonlinear creep damage con-stitutive model of salt rock based on multistage creep test: Implications for underground natural gas storage in salt cavern. *Energy Sci. Eng.* **2020**, *8*, 1592–1603. [CrossRef]
28. Lin, Y.X.; Yin, Z.Y.; Wang, X.; Huang, L.C. A systematic 3D simulation method for geomaterials with block inclusions from image recognition to fracturing modelling. *Theor. Appl. Fract. Mech.* **2022**, *117*, 103194. [CrossRef]
29. Zhao, Y.L.; Zhang, L.Y.; Wang, W.J.; Pu, C.Z.; Wan, W.; Tang, J.Z. Cracking and stress-strain behavior of rock-like material containing two flaws under uniaxial compression. *Rock Mech. Rock Eng.* **2016**, *49*, 2665–2687. [CrossRef]
30. Liu, G.C.; Huang, X.; Pang, J.Y. The uniaxial creep characteristics of red sandstone under dry-wet cycles. *Adv. Civ. Eng.* **2020**, *2020*, 8841773. [CrossRef]
31. Wang, Z.; Shen, M.R.; Gu, L.L.; Zhang, F. Creep behavior and long-term strength characteristics of greenschist under different confining pressures. *Geotech. Test. J.* **2017**, *41*, 20170143. [CrossRef]
32. Li, S.N.; Huang, Z.H.; Liang, Q.; Liu, J.; Luo, S.L.; Zhou, W.Q. Evolution Mechanism of Mesocrack and Macrocrack Propagation in Carbonaceous Mudstone under the Action of Dry-Wet Cycles. *Geofluids* **2022**, *2022*, 6768370. [CrossRef]
33. Zhao, Y.; Li, J.T.; Ma, G. Experimental study on the damage and degradation characteristics of red sandstone after dry and wet cycling by low magnetic field nuclear magnetic resonance (NMR) technique. *Geofluids* **2021**, *2021*, 8866028. [CrossRef]
34. Zhang, F.R.; Jiang, A.N.; Yang, X.Y. Shear creep experiments and modeling of granite under dry-wet cycling. *Bull. Eng. Geol. Environ.* **2021**, *80*, 5897–5908. [CrossRef]
35. Lin, Y.X.; Wang, X.; Ma, J.J.; Huang, L.C. A systematic approach for modelling the hydraulic fracturing of rocks with irregular inclusions using a combined finite-discrete method. *Eng. Fract. Mech.* **2022**, *261*, 108209. [CrossRef]
36. Zhao, Y.L.; Wang, Y.X.; Tang, L.M. The compressive-shear fracture strength of rock containing water based on Druker-Prager failure criterion. *Arab. J. Geosci.* **2019**, *12*, 452. [CrossRef]
37. Zhao, Y.; Zhang, L.; Wang, W.; Wan, W.; Ma, W. Separation of elastoviscoplastic strains of rock and a nonlinear creep model. *Int. J. Geomech.* **2018**, *18*, 04017129. [CrossRef]
38. Jia, C.J.; Xu, W.Y.; Wang, R.B.; Wang, S.S.; Lin, Z.N. Experimental investigation on shear creep properties of undisturbed rock discontinuity in Baihetan Hydropower Station. *Int. J. Rock Mech. Min. Sci.* **2018**, *104*, 27–33. [CrossRef]
39. Zhao, Y.L.; Liu, Q.; Lian, J.; Wang, Y.X.; Tang, L.M. Theoretical and numerical models of rock wing crack subjected to hydraulic pressure and far-field stresses. *Arab. J. Geosci.* **2020**, *13*, 926. [CrossRef]